Low-temperature magnetron sputter-deposition, hardness, and electrical resistivity of amorphous and crystalline alumina thin films

Quan Li
Department of Materials Science and Engineering, Northwestern University, Evanston, Illinois 60208

Yuan-Hsin Yu
Department of Materials Engineering, Tatung University, Taipei, Taiwan, Republic of China

C. Singh Bhatia
IBM Storage Systems Division, 5600 Cottle Road, San Jose, California 95193

L. D. Marks
Department of Materials Science and Engineering, Northwestern University, Evanston, Illinois 60208

S. C. Lee
Department of Materials Engineering, Tatung University, Taipei, Taiwan, Republic of China

Y. W. Chung[a)]
Department of Materials Science and Engineering, Northwestern University, Evanston, Illinois 60208

(Received 7 October 1999; accepted 12 May 2000)

Aluminum oxide films were grown by reactive magnetron sputtering. In order to maintain a stable deposition process and high deposition rate, a pulsed direct current bias was applied to the aluminum target and the substrate. An external solenoid was used to form a magnetic trap between the target and the substrate. The influence of substrate temperature, substrate bias, and the magnetic trap on film growth and properties was studied by different surface and thin-film analysis techniques and electrical measurements. Normally, amorphous alumina films were produced. However, under optimum process conditions, crystalline alumina films can be obtained at temperatures as low as 250 °C, with a hardness ~20 GPa and excellent electrical insulating properties. © *2000 American Vacuum Society.* [S0734-2101(00)04605-4]

I. INTRODUCTION

Aluminum oxide thin films have many properties that are useful for applications in optical electronics, and cutting tool industries. Methods of synthesizing aluminum oxide thin films include chemical vapor deposition combined with ion-beam irradiation,[1] molecular beam epitaxy using a solid aluminum source and N_2O,[2] laser-induced deposition from condensed layers of organoaluminum compounds and water,[3] and magnetron sputter deposition.[4]

Traditional radio frequency (rf) sputtering uses an aluminum oxide target and generally results in low deposition rates. Direct current (dc) reactive sputtering of aluminum in an oxygen/argon atmosphere can produce stoichiometric Al_2O_3 at high rates. The major requirement is careful control of the oxygen partial pressure[5] so that the aluminum target will not be poisoned. In addition, pulsed dc magnetron sputtering was used in recent years to minimize arcing during deposition of insulating materials such as alumina.[6] In this case, the magnetron target voltage was bipolar at a certain frequency (2–30 kHz typically). In the positive cycle, electrons travel towards the target and neutralize the positive charge accumulated on the target surface in the negative cycle. When this is done properly and at sufficiently high frequency, one obtains a stable, arc-free magnetron plasma.

Generally, one needs to use substrate temperatures higher than 700 °C to obtain crystalline alumina.[7] This high substrate temperature requirement limits the type of substrates that can be coated with alumina. Therefore, low-temperature synthesis of crystalline alumina is of great technological interest. One method to reduce the crystalline growth temperature is to enhance the mobility of surface species via low-energy ion bombardment. To explore this strategy, Schneider *et al.*[8] incorporated a rf coil to enhance ionization in a standard magnetron sputter-deposition system. Together with pulsed dc substrate bias to enhance ion bombardment of the growing film, they demonstrated the growth of crystalline κ alumina at relatively low substrate temperatures (400 °C).

In this study, we report the synthesis and properties of aluminum oxide thin films grown by pulsed dc magnetron sputtering. Instead of using a rf coil to increase the ion concentration in the plasma, we used a magnetron sputter source equipped with strong magnets instead. An additional magnetic field with the correct polarity was applied near the substrate to form a magnetic trap. With proper substrate biasing, this results in markedly improved ion currents to the substrate during film growth, as demonstrated by Petrov *et al.*[9] and Engstrom *et al.*[10]

II. EXPERIMENTAL PROCEDURES

Aluminum oxide films were grown using pulsed dc magnetron sputtering in a single-cathode deposition chamber (Fig. 1). The base pressure of the chamber was below 1×10^{-7} Torr. We used a 2 in. aluminum target (99.99% purity) in an unbalanced magnetron. The target voltage was pulsed at 20 kHz (50% duty cycle), with the positive voltage set at 10% of the negative voltage (e.g., at a set target bias of

[a)]Electronic mail: ywchung@nwu.edu

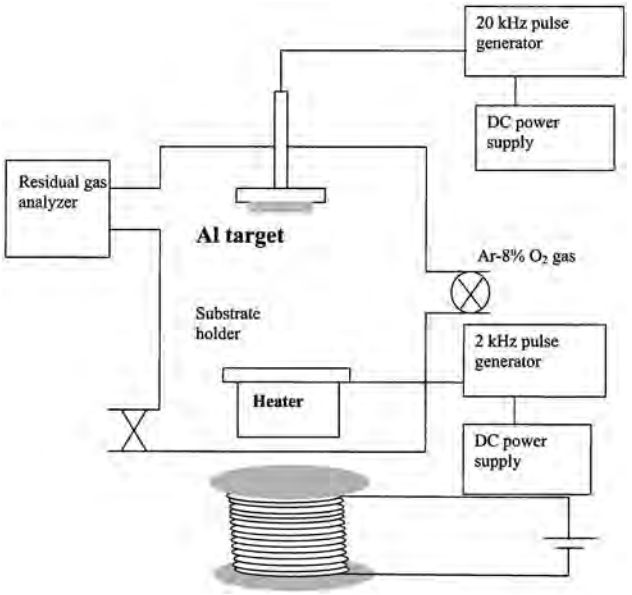

FIG. 1. Schematic diagram of the deposition chamber.

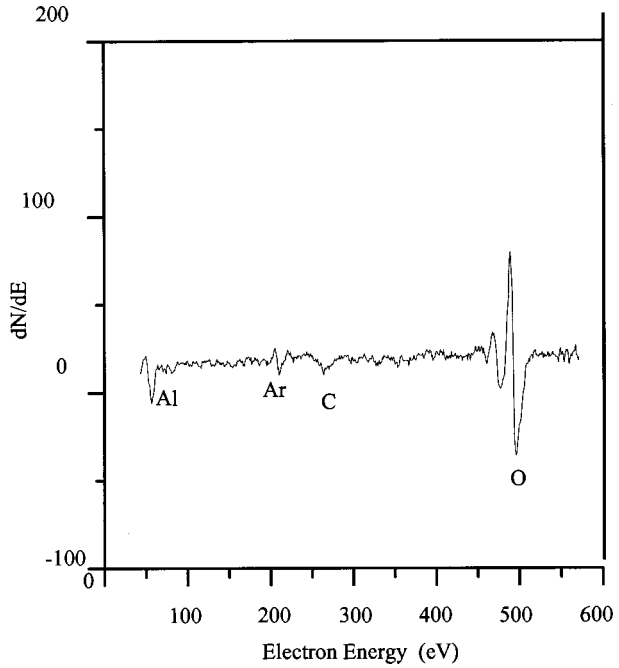

FIG. 2. Auger electron spectrum of a typical alumina film deposited on Si. The Al Auger peak is 51 eV, characteristic of oxidized Al.

−400 V, the actual target voltage is a rectangular wave cycling between −400 and +40 V). The sputtering gas was an argon-8% oxygen mixture at a total pressure of 7 mTorr. Si(100) wafers were used as substrates. They were first cleaned by acetone and 2-propanol, then transferred into the chamber and reverse-sputter etched in an argon plasma at 60 mTorr. In selected runs, glass substrates were used to confirm visually the stoichiometry of alumina films (stoichiometric alumina films should be transparent). A 2 kHz pulsed dc bias (similar pulse shape as that applied to the target) was applied to the substrate during deposition for low-energy ion bombardment and eliminating charging. This bias was varied from −200 to −400 V. Substrate temperatures were maintained at or below 300 °C, as measured by a thermocouple attached to the substrate holder. A magnetic field was applied (via an external solenoid) during deposition to further increase the substrate ion-current density. The field at the substrate surface was 42 G. Unless otherwise stated, the thickness of all films was 300 nm.

Auger electron spectroscopy was used to examine the chemical composition of the films. Film structure was characterized by standard x-ray diffraction using the Cu $K\alpha$ line (0.154 nm) and transmission electron microscopy (TEM). The surface topography was obtained by atomic force microscopy (AFM). The film hardness was measured using a Hysitron nanoindentor, analyzed by the Pharr–Oliver method.[11] In the latter case, the penetration was kept at less than 15% of the film thickness to minimize substrate effects. Film stress was measured using the wafer curvature method. Through-thickness dc electrical resistivity was also determined.

III. RESULTS AND DISCUSSION

A. Appearance

At a nominal target power of 100 W, deposition under conditions described in the previous section resulted in clear alumina films at 5 nm/min on substrates 13 cm from the target. Auger electron spectroscopy showed that the aluminum in the films gives an Auger peak at 51 eV, confirming that it is in an oxidized state (Fig. 2).

B. Substrate temperature effect

To examine the effect of substrate temperature on the growth of alumina, we deposited three films at the same nominal power (100 W), pulsed substrate bias (−300 V) and with the external solenoid on, but with different substrate temperatures, *viz.*, 200, 250, and 300 °C. X-ray diffraction (Fig. 3) showed that crystalline alumina films can be grown at 250 and 300 °C and appear to consist of mixed phases. For example, the peak at ~25° suggests the presence of α alumina, while the peak at ~30° can be due to either θ or κ phase. Because of stress-induced shifting of diffraction peaks and nonrandom texture, we are unable to make specific phase identification and composition analysis at this time. The reference powder patterns for four typical alumina phases are included in this and other x-ray diffraction patterns.[12] The alumina film grown at 200 °C is amorphous [the Si(200) forbidden reflection appears because of growth-induced stress].

For the film grown at 300 °C, high-resolution TEM images were taken at the Si substrate/film interface (Fig. 4), as well as regions away from the interface (Fig. 5) with the electron beam along the substrate [110] direction. Fringes in the aluminum oxide region are indicative of its crystalline nature. This is also confirmed by the ring diffraction pattern taken from the same region of the film. Figure 6 shows that some amorphous regions still exist.

Crystalline films grown at ≥250 °C have nanoindentation hardness 18–21 GPa, in the same range as crystalline α alu-

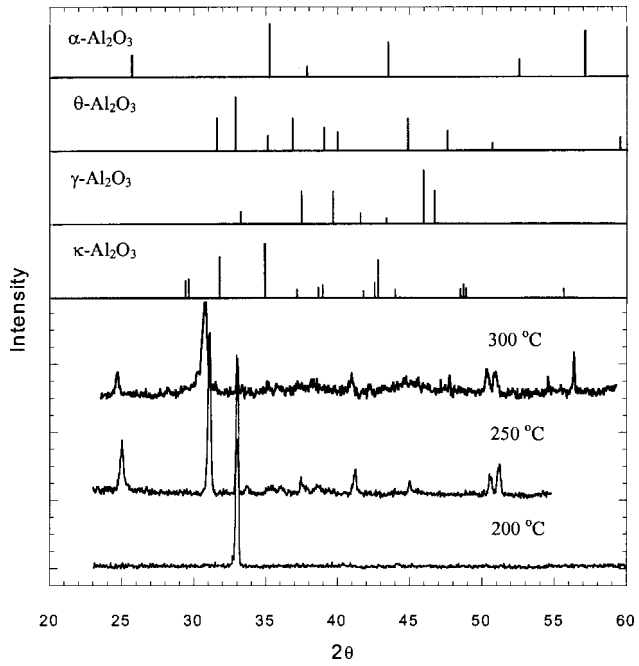

FIG. 3. High-angle x-ray diffraction patterns of aluminum oxide films deposited at 200, 250, and 300 °C (nominal target power=100 W, pulsed substrate bias=−300 V, magnetic field on). The Si (200) forbidden reflection at $2\theta=33°$ appears because of stress.

mina (sapphire). For amorphous films grown at 200 °C, the hardness is 12 GPa or less.

C. Substrate bias effect

In this series of experiments, we kept the nominal target power and substrate temperature constant (100 W and 300 °C, respectively), with the external solenoid on. The substrate bias was set at −200, −300, and −400 V. Crystalline alumina films were obtained at −300 and −400 V substrate bias, while films grown at −200 V were amorphous (Fig. 7). Alumina films grown at 300 V substrate bias appear to have better quality than those at −400 V. The diffraction peaks are stronger, and the films are harder (20.7 vs 17.6 GPa). AFM indicates (Fig. 8) that films grown at −300 V are smoother [root-mean-square (rms) surface roughness=0.36 nm] than those grown at −400 V (rms surface roughness =1.78 nm).

Substrate bias has two opposing effects on crystal growth. On the one hand, substrate bias increases ion bombardment of the growing film, enhancing mobility of surface species. This makes it possible to grow crystalline alumina films at reduced temperatures. On the other hand, excessive ion bombardments can create defects at higher rates than can be repaired by enhanced mobility of surface species. Further, excessive compressive stress can result. Therefore, some optimum bias must be found.

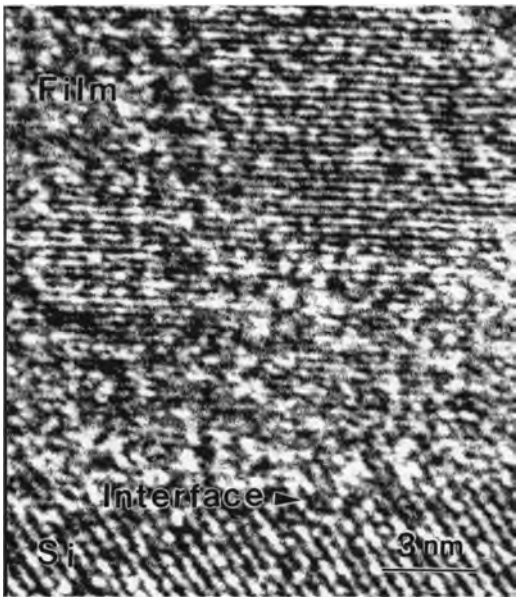

FIG. 4. High-resolution TEM image taken at the interface of Si and aluminum oxide with the electron beam along the Si [110] direction for the film shown in Fig. 3 (substrate temperature=300 °C). Fringes in the aluminum oxide region are evident, indicative of crystalline growth.

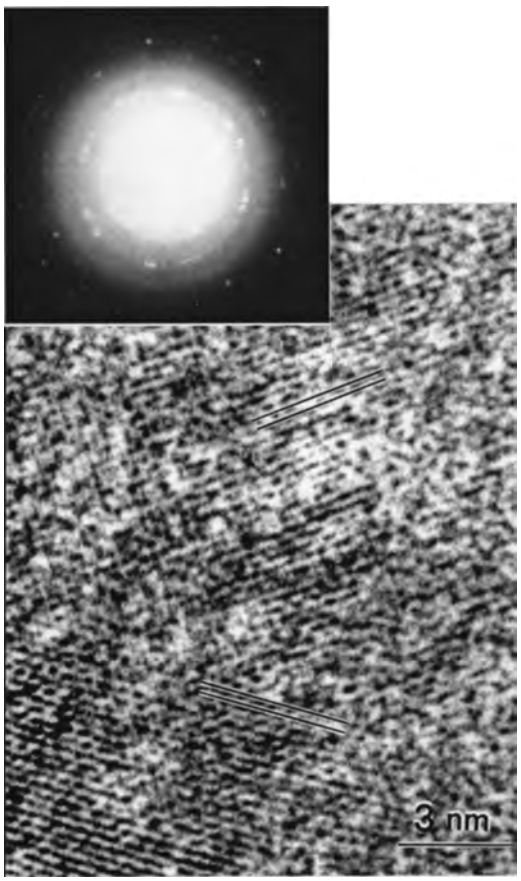

FIG. 5. High-resolution TEM image taken at the film region away from the film/substrate interface for the film shown in Fig. 3 (substrate temperature =300 °C). Randomly oriented aluminum oxide grains can be seen. The ring diffraction pattern in the inset shows a presence of polycrystalline aluminum oxide.

D. Magnetic field effect and amorphization

The next series of films were grown at a nominal target power of 100 W, substrate bias of −300 V, and substrate

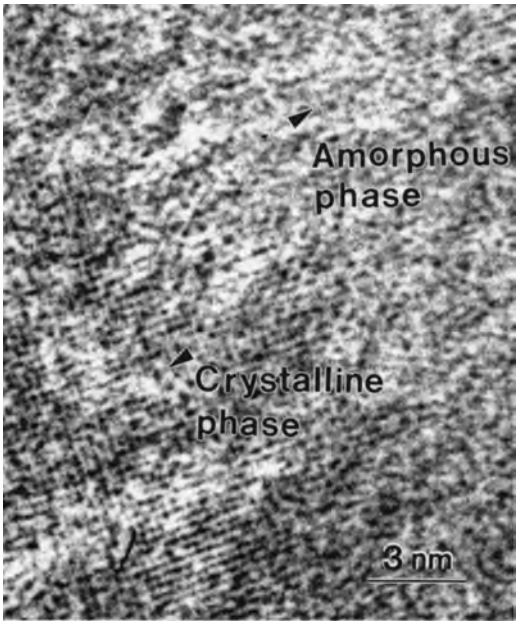

FIG. 6. High-resolution TEM image taken at the film region away from the film/substrate interface for the film shown in Fig. 3 (substrate temperature =300 °C). Both crystalline and amorphous phases are observed.

temperature 300 °C, one set with the solenoid off and one set with the solenoid on. Separate measurements under the same process conditions showed that the ion-to-neutral arrival ratio at the substrate is 2.7 with the solenoid off and 5.2 on.[13]

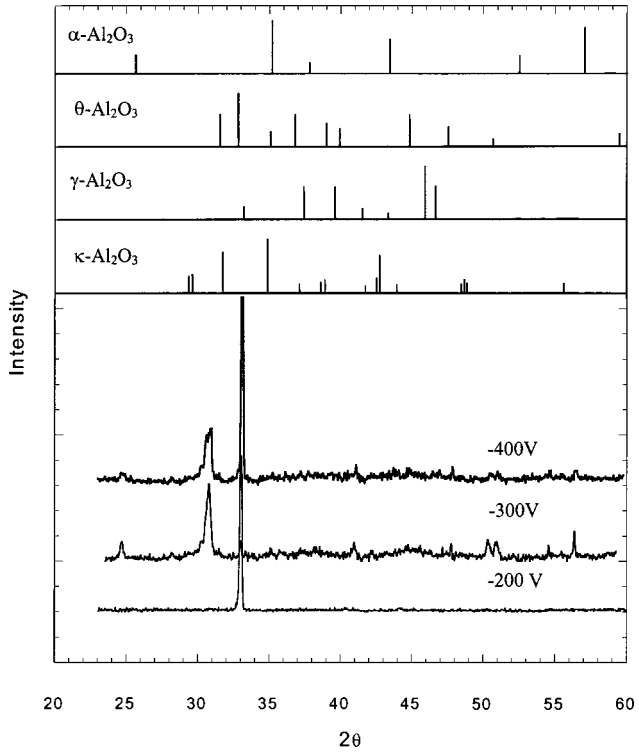

FIG. 7. High-angle x-ray diffraction patterns of aluminum oxide films deposited at −200, −300, and −400 V substrate bias (nominal target power =100 W, substrate temperature=300 °C, magnetic field on). Crystalline phases are obtained at −300 and −400 V.

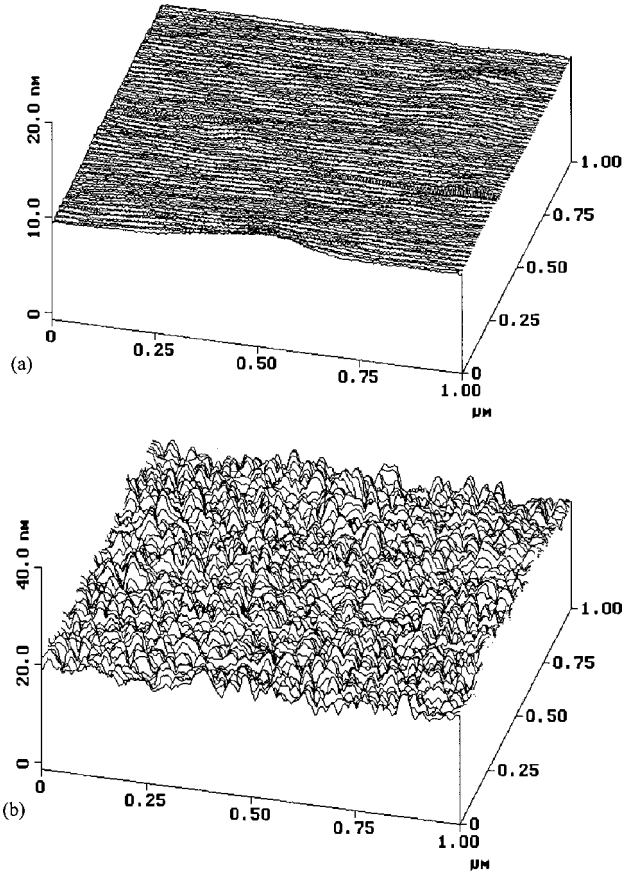

FIG. 8. AFM images of aluminum films deposited at different substrate bias voltages (nominal target power=100 W, substrate temperature=300 °C, magnetic field on). (a) Substrate bias=−300 V, rms surface roughness =0.36 nm and (b) Substrate bias=−400 V, rms surface roughness=1.78 nm.

This approximate doubling of the ion-to-neutral arrival ratio has a dramatic effect on film crystallinity. Figure 9 shows that without the magnetic field provided by the solenoid, there is no crystalline growth.

Together with the substrate bias, formation of a magnetic trap above the substrate surface increases ion bombardment of the growing film. As discussed earlier, this can enhance crystalline growth under optimum bias conditions. At the same time, such ion bombardment results in significantly increased film stress. For example, films grown with the solenoid on (Fig. 9) have internal compressive stress ~5 GPa, whereas films grown with the solenoid off have internal stress ~1 GPa. While thin crystalline alumina films appear to be stable (from electrical resistivity measurements), thick (>100 nm) crystalline films grown under these conditions experienced partial amorphization 5–7 days after film deposition (as shown by the marked decrease of x-ray diffraction intensity). This occurs even for films stored in a dessicator, suggesting that moisture is not a significant factor here.

E. Resistivity

Through-thickness electrical resistivity of amorphous alumina films was measured as a function of the applied electric

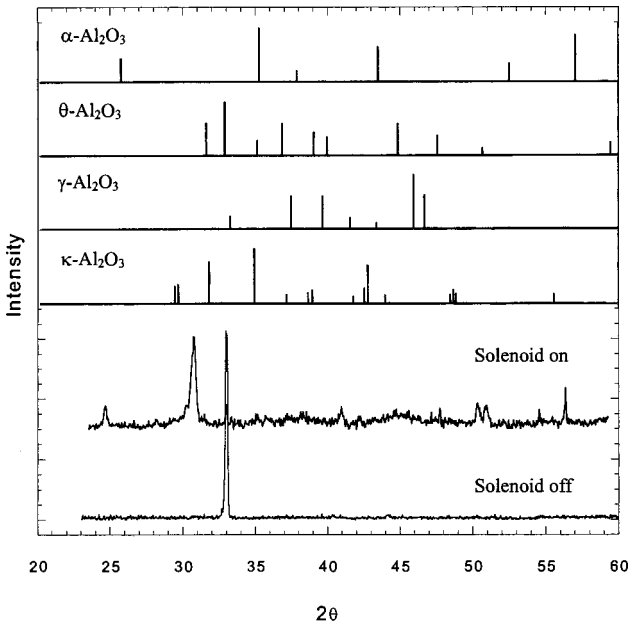

FIG. 9. High-angle x-ray diffraction patterns of aluminum oxide films grown with and without the extra magnetic field (nominal target power=100 W, substrate bias=−300 V, substrate temperature=300 °C). Crystalline alumina appears only when the field is on.

field, film thickness ranging from 10 to 50 nm (100 W nominal target power, −250 V substrate bias, with the solenoid off). There was no deliberate substrate heating. The substrate temperature was in the range of 100 °C. Figure 10 shows two general trends. First, the resistivity decreases with increasing film thickness. This is most likely due to the classical size effect. Second, the resistivity decreases with increasing electrical field. We speculate that this may be due to tunneling between conducting (defective) regions in the film. The detailed mechanism is beyond the scope of our investigation. Another way to view the data is that all alumina films exhibit no through-thickness breakdown and maintain resistivity $>10^9\ \Omega\,\mathrm{cm}$ upon application of 10 V.

Figure 11 shows the resistivity data for three alumina films (10 nm amorphous, 3 nm crystalline, and 10 nm crystalline). The crystalline films were grown at 100 W nominal target power, −300 V substrate bias, 300 °C substrate temperature and with the solenoid on. Except at the lowest electric fields, crystalline alumina films generally have higher and more stable resistivity than amorphous ones with increasing electric field. This may be the result of crystalline alumina films having lower defect concentrations. These results indicate that ultrathin alumina films may be useful for low-voltage electrical isolation applications.

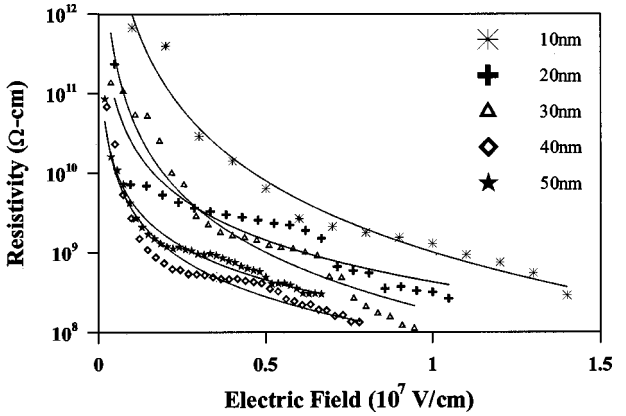

FIG. 10. Variation of through-thickness electrical resistivity with applied electric field for amorphous alumina films (nominal target power=100 W, substrate bias=−250 V, substrate temperature=100 °C, magnetic field off).

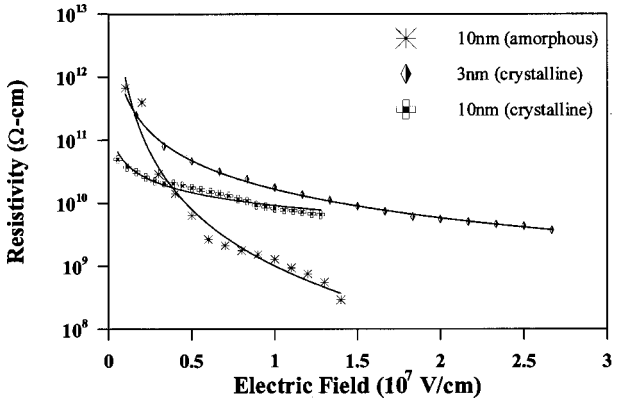

FIG. 11. Variation of through-thickness electrical resistivity with applied electric field for amorphous and crystalline alumina films. The two crystalline films were grown at 100 W nominal target power, −300 V substrate bias, 300 °C substrate temperature and with the magnetic field on.

IV. CONCLUSIONS

We demonstrate that stoichiometric alumina thin films can be synthesized by reactive magnetron sputtering with pulsed dc bias applied to the target and the substrate. Normally, amorphous films were produced with hardness <12 GPa and high electrical resistivity. Under optimum process conditions and the formation of a magnetic trap between the target and the substrate, crystalline alumina films can be grown at substrate temperatures as low as 250 °C. The hardness is comparable to crystalline α alumina. Excellent electrical properties are maintained down to a thickness of 3 nm.

ACKNOWLEDGMENTS

This work was supported by the MRSEC program of the National Science Foundation (DMR-9632472) at the Materials Research Center of Northwestern University and the IBM Storage System Division.

[1]H. Nakai, J. Shinohara, T. Sassa, and Y. Ikegami, Nucl. Instrum. Methods Phys. Res. B **121**, 125 (1997).
[2]H. Wado, T. Shimizu, and M. Ishida, Appl. Phys. Lett. **67**, 2200 (1995).
[3]J. F. Moore, D. R. Strongin, P. B. Comita, M. W. Ruckman, and Myron Strongin, Appl. Phys. Lett. **65**, 368 (1994).
[4]C. Deshpandey and L. Holland, Thin Solid Films **96**, 265 (1982).
[5]W. D. Sproul, M. E. Graham, M. S. Wong, S. Lopez, D. Li, and R. A. Scholl, J. Vac. Sci. Technol. A **13**, 1188 (1995).
[6]M. S. Wong, W. J. Chia, P. Yashar, J. M. Schneider, W. D. Sproul, and S. A. Barnett, Surf. Coat. Technol. **86–87**, 381 (1996).
[7]B. Hirschauer, S. Soderholm, G. Chiaia, and U. O. Karlsson, Thin Solid Films **305**, 243 (1997).

[8]J. M. Schneider, W. D. Sproul, A. A. Voevodin, and A. Matthews, J. Vac. Sci. Technol. A **15**, 1 (1997).
[9]I. Petrov, F. Adibi, J. E. Greene, W. D. Sproul, and W. D. Munz, J. Vac. Sci. Technol. A **10**, 3283 (1992).
[10]C. Engstrom, T. Berlind, J. Birch, L. Hultman, I. P. Ivanov, S. R. Kirkpatrick, and S. Rohde, Vacuum **56**, 107 (2000).
[11]G. M. Pharr and W. C. Oliver, Mater. Res. Bull. **17**, 28 (1992).
[12]Standard powder x-ray diffraction patterns in Figs. 3, 7, and 9 include peaks with intensity >10% of the strongest peak for that phase. References for α, θ, and γ alumina are 1997 JCPDS 46-1212, 1997 JCPDS 35-0121, and 1998 JCPDS 47-1308. Reference for κ alumina is M. Halvarsson, V. Langer, and S. Vuorinen, Powder Diffr. **14**, 61 (1999).
[13]The ion-to-neutral arrival ratio was calculated as follows. The deposition rate is 300 nm/h, or 1000 monolayers/h (assuming 0.3 nm=1 monolayer). Assuming a surface atom density of 1×10^{15} atoms/cm^2, this is equivalent to an atom arrival rate of 2.78×10^{14} atoms/cm^2 s. The substrate ion current density was measured to be 0.12 mA/cm^2 with the solenoid off, and 0.23 mA/cm^2 with the solenoid on. Assuming singly charged ions, we calculated ion arrival rates of 7.5×10^{14} and 1.44×10^{15} ions/cm^2 s respectively. The corresponding ion-to-neutral arrival rates are then 2.7 and 5.2.